Available online at www.sciencedirect.com
ScienceDirect
Geochimica et Cosmochimica Acta 70 (2006) 5571–5582
Geochimica
www.elsevier.com/locate/gca

Solubilities of corundum, wollastonite and quartz in H_2O–NaCl solutions at 800 °C and 10 kbar: Interaction of simple minerals with brines at high pressure and temperature

Robert C. Newton, Craig E. Manning *

Department of Earth and Space Sciences, University of California Los Angeles, Los Angeles, CA 90095-1567, USA

Received 23 February 2006; accepted in revised form 14 August 2006

Abstract

Solubilities of corundum (Al_2O_3) and wollastonite ($CaSiO_3$) were measured in H_2O–NaCl solutions at 800 °C and 10 kbar and NaCl concentrations up to halite saturation by weight-loss methods. Additional data on quartz solubility at a single NaCl concentration were obtained as a supplement to previous work. Single crystals of synthetic corundum, natural wollastonite or natural quartz were equilibrated with H_2O and NaCl at pressure (P) and temperature (T) in a piston-cylinder apparatus with NaCl pressure medium and graphite heater sleeves. The three minerals show fundamentally different dissolution behavior. Corundum solubility undergoes large enhancement with NaCl concentration, rising rapidly from Al_2O_3 molality ($m_{Al_2O_3}$) of 0.0013(1) (1σ error) in pure H_2O and then leveling off to a maximum of ~0.015 at halite saturation ($X_{NaCl} \approx 0.58$, where X is mole fraction). Solubility enhancement relative to that in pure H_2O, $X_{Al_2O_3}/X^{\circ}_{Al_2O_3}$, passes through a maximum at $X_{NaCl} \approx 0.15$ and then declines towards halite saturation. Quenched fluids have neutral pH at 25 °C. Wollastonite has low solubility in pure H_2O at this P and T ($m_{CaSiO_3} = 0.0167(6)$). It undergoes great enhancement, with a maximum solubility relative to that in H_2O at $X_{NaCl} \approx 0.33$, and solubility >0.5 molal at halite saturation. Solute silica is 2.5 times higher than at quartz saturation in the system H_2O–NaCl–SiO_2, and quenched fluids are very basic (pH 11). Quartz shows monotonically decreasing solubility from $m_{SiO_2} = 1.248$ in pure H_2O to 0.202 at halite saturation. Quenched fluids are pH neutral. A simple ideal-mixing model for quartz-saturated solutions that requires as input only the solubility and speciation of silica in pure H_2O reproduces the data and indicates that hydrogen bonding of molecular H_2O to dissolved silica species is thermodynamically negligible. The maxima in $X_{Al_2O_3}/X^{\circ}_{Al_2O_3}$ for corundum and wollastonite indicate that the solute products include hydrates and Na^+ and/or Cl^- species produced by molar ratios of reactant H_2O to NaCl of 6:1 and 2:1, respectively. Our results imply that quite simple mechanisms may exist in the dissolution of common rock-forming minerals in saline fluids at high P and T and allow assessment of the interaction of simple, congruently soluble rock-forming minerals with brines associated with deep-crustal metamorphism.

1. Introduction

Fluid inclusions in rocks of deep-seated origin give indication of the complexity of fluid activity in the earth's interior. Fluid compositions approaching pure H_2O are rarely observed; instead, the fluids trapped in minerals of peridotites, granulites and eclogites are usually CO_2-rich (Touret, 1971; Roedder, 1972) and may be very salty, with daughter crystals of chloride, sulfate, oxide and silicate minerals (e.g., Philippot and Selverstone, 1991; Smit and Van Reenen, 1997). Some high-pressure granulite terranes feature both carbonic and salty fluid inclusions, apparently captured coevally during deep-crustal metamorphism (Touret, 1985; Crawford and Hollister, 1986). These observations predict substantial immiscibility between CO_2-rich and saline aqueous fluids even at quite elevated P and T, as deduced from experimental fluid-inclusion studies (Johnson, 1991; Gibert et al., 1998; Shmulovich and Graham, 2004).

Possible roles of complex fluids in metamorphism, metasomatism, and mineralization have been debated. H_2O

* Corresponding author. Fax: +1 310 825 2779.
E-mail address: manning@ess.ucla.edu (C.E. Manning).

0016-7037/$ - see front matter © 2006 Elsevier Inc. All rights reserved.
doi:10.1016/j.gca.2006.08.012

activity in deep-crustal metamorphism must be quite low in order to prevent widespread hydration reactions, or, at higher temperatures, rock melting. Estimates of H_2O activity in granulite facies metamorphism based on hydrous mineral equilibria range from 0.15 (Valley et al., 1983) to 0.4–0.5 (Aranovich et al., 1987); more modern estimates based on experimental revision of phlogopite stability indicate that the higher values may be generally more appropriate (Aranovich and Newton, 1998). The amount of such fluids which typically participated in deep-crustal metamorphism is also debated. Some authors suggest that fluid action typically is negligible (Lamb and Valley, 1984), whereas others have found evidence that fluid effects in some high-grade metamorphic episodes have been large (Ague, 1994; Manning and Ingebritsen, 1999). Evidence from stable isotope alteration in some granulites indicates that fluid masses which interacted with rocks must have been quite small, perhaps only a fraction of the rock masses they interacted with (Valley et al., 1990). Newton et al. (1998) showed, however, that very small fluid-to-rock ratios could account for dehydration of biotite to form orthopyroxene during granulite facies metamorphism, and Newton and Manning (2005) demonstrated that quite small amounts of saline fluids with a high sulfate content could account for the wide-spread oxidation known to have affected some exposed deep-crustal terranes (e.g. Cameron and Hattori, 1994).

Lack of experimental information has hampered interpretation of fluid action at deep-crust and upper mantle conditions. Most of the existing experimental work relates to fluids at low P and T near the critical point of H_2O, where the solution behavior is quite complex. A vivid demonstration of this is the solubility of quartz in the low pressure range. At 0.5 kbar, the temperature coefficient of solubility changes from positive to negative over the range 300–500 °C (Kennedy, 1950). Calculations of phase equilibria and component activities in the simple system H_2O–NaCl at pressures below 2 kbar (where NaCl is partly to strongly associated) require complex algorithms (Bowers and Helgeson, 1983). Quartz solubility in H_2O–NaCl fluids undergoes strong increase with increasing salinity at 1–2 kbar (Novgorodov, 1977; Xie and Walther, 1993; Newton and Manning, 2000; Shmulovich et al., 2006). If solute silica exists as a neutral monomeric dihydrate with additional hydrogen-bonded water molecules (e.g., Walther and Orville, 1983), decrease of H_2O activity in H_2O–NaCl fluids should inhibit quartz solubility, as it does in H_2O–CO_2 and H_2O–Ar fluids (Walther and Orville, 1983), unless there is strong interaction of quartz with NaCl-bearing fluids in the low-pressure range, perhaps with the formation of Na-silicate or Si chloride species. Anderson and Burnham (1967) suggested the reaction:

$$\underset{\text{quartz}}{SiO_2} + 2H_2O + NaCl = H_3NaSiO_{4,aq} + HCl \quad (1)$$

Measurements at elevated P and T suggest that chloride solutions, and quartz solubility in them, are much simpler than at shallow-crustal conditions (Aranovich and Newton, 1996, 1997; Newton and Manning, 2000; Shmulovich et al., 2001, 2006; Tropper and Manning, 2004). Aranovich and Newton (1996) found that at 650–850 °C and 10–15 kbar, the activities of H_2O and NaCl are closely approximated by a simple mixing model involving fully dissociated NaCl, in which Na^+ and Cl^- ions mix ideally with H_2O molecules. This ideal-fused-salt model, advocated by Bradley (1962) for melting of hydrated salt mixtures at high T and P, leads to the simple expressions for component activities

$$a_{H_2O} = (1 - X_{NaCl})/(1 + X_{NaCl}) \quad (2a)$$

$$a_{NaCl} = 4X_{NaCl}^2/(1 + X_{NaCl})^2 \quad (2b)$$

where X_{NaCl} is the mole fraction of NaCl. Moreover, quartz solubility in such fluids is also simpler than at low P and T. Newton and Manning (2000) found that above 7 kbar, the solubility of quartz decreases monotonically with NaCl concentration. This implies that solvent interaction is much weaker at high pressures, probably due to destabilization of hydrated aqueous silica by decreasing H_2O activity. Finally, Zotov and Keppler (2002) and Newton and Manning (2003) found that quartz solubility and silica activity in aqueous fluids could be described accurately by an ideal solution model in which silica monomers ($H_4SiO_4 \cdot$ solvated H_2O) and dimers ($H_6Si_2O_7 \cdot$ solvated H_2O) mix ideally with H_2O molecules. These observations suggest that insight into the interaction of minerals with complex natural fluids may be gained from simple mixing considerations once accurate solubility data at high P and T are compiled for a number of common minerals.

The present study investigates the solubilities of corundum and wollastonite at 800 °C and 10 kbar, and NaCl mole fraction (X_{NaCl}) from zero to halite saturation (~0.58; Aranovich and Newton, 1996). Previous work on the solubilities of these minerals is too scant to draw general conclusions about dissolution reactions in H_2O–NaCl at high T and P. Anderson and Burnham (1967) made a few reconnaissance experiments on the solubility of corundum in moderately concentrated NaCl solutions at 700 °C and pressures up to 4 kbar. They suggested that NaCl enhances corundum solubility, but did not establish the magnitude of the effect. Walther (2001) found that NaCl concentrations up to 1 molal (1.8 mol%) enhances corundum solubility at pressures up to 2 kbar and temperatures to 500 °C. These data cannot be extrapolated to higher P and T: the possibility exists that NaCl enhancement of corundum solubility behaves like that of quartz, and that pressure increase beyond 2 kbar reverses the initial solubility enhancement. No experimental data on the solubility of wollastonite in NaCl solutions were available prior to the present study. The only comprehensive data on quartz in NaCl solutions at elevated P and T are those of Newton and Manning (2000) and Shmulovich et al. (2001). The two data sets are in reasonable agreement: they show monotonic decrease of quartz solubility with NaCl

concentration at pressures greater than 5 kbar. These data, together with the present data for corundum and wollastonite, provide a framework for a first assessment of the physical chemistry of dissolution reactions of minerals in concentrated brines at deep-seated conditions.

2. Experimental methods

Starting materials were single crystals of high-purity synthetic corundum and natural wollastonite and quartz, reagent NaCl and doubly distilled, deionized H_2O. Two types of corundum were used. Chips of 1–7 mg weight from a large corundum boule were shaped into ellipsoids with a diamond file and smoothed with 600-mesh alundum paper and 15 μm diamond paper. Fig. 1a shows the appearance of a typical corundum starting crystal. A few solution experiments were made with synthetic corundum spheres of about 32 mg, obtained from P. Tropper (U. Innsbruck) and used in the study of Tropper and Manning (2005b). The wollastonite starting material was a very pure natural sample used in the solution calorimetry study of Charlu et al. (1978). Quartz starting material was the natural sample used by Newton and Manning (2000).

Experimental materials were encapsulated in welded segments of Pt tubing of 3.5 mm diameter and 0.15 mm wall thickness. It was necessary to encapsulate the somewhat fragile wollastonite crystals in inner Pt capsules of 1.5 mm diameter, perforated with 3–7 small holes to allow access of the fluid. Materials were loaded into the large Pt capsules in the order: crystal (or inner capsule), NaCl, H_2O, with weighing at each step. The capsule was then sealed by arc welding.

All experiments were performed in the 3/4-in. (1.91-cm) diameter piston-cylinder apparatus with NaCl pressure medium and graphite heater sleeve. Pressure was measured with a Heise Bourdon-tube gauge which was calibrated against a highly accurate standard gauge. All experiments were made in the piston-out mode: first, an assembly was brought to a nominal pressure of 7 kbar, then heated to 800 °C. Thermal expansion of the assembly carried the pressure to 10 kbar; some bleeding of oil pressure was needed to prevent overshooting. Pressures are considered accurate to ±300 bars. Temperatures were measured and controlled automatically with calibrated matched pairs of $W_{97}Re_3$ vs. $W_{75}Re_{25}$ thermocouples in contact with the sample capsules and are considered accurate to ±3 °C.

Experiments were quenched by cutting power to the apparatus. Temperature fell below 200 °C in ~10 s. After extraction of the capsule from the assembly, the H_2O contents were in most cases checked by drying weight loss and found to agree with the initial H_2O within 0.6 wt%. In several experiments, the pH of the quench fluid was determined using pH paper calibrated in integer increments. The paper strip was placed face-down on a cleaned quenched capsule and the puncturing needle penetrated both paper and capsule. The indicator squares were thoroughly wetted as the capsule fluid oozed out, and the color-code was read while still wet. When pH of quench fluid was determined it was not possible to determine the H_2O weight after an experiment. For consistency, we therefore used H_2O-in weight in solubility calculations where possible.

Solubilities were determined by weight losses of the crystals, or, for wollastonite, by weighing both inner capsule and residual crystal from a quenched experiment. Masses of corundum before and after most experiments, as well as H_2O and NaCl in all runs, were determined on a Mettler M3 microbalance, for which $1\sigma = 2$ μg for each reported weight based on repeated weighings of a standard. Masses so determined are reported in Table 1 to three decimal places; i.e., to the nearest microgram. During the course of this study we switched to a Mettler UMX2 ultramicrobalance ($1\sigma = 0.2$ μg) for crystal and inner-capsule weighings. Table 1 gives these higher precision weights to four decimal places. Concentrations are reported on the molality scale (moles solute per kg H_2O) assuming that any H_2O removed from the bulk solvent to form hydrous solutes is negligible.

In the wollastonite experiments, the quenched and dried NaCl precipitate was removed from an inner capsule by soaking in H_2O at 80 °C for 10-min periods, followed by drying, until constant weight was attained. A small amount of insoluble quench residue in the inner capsule consisted of myriad tiny siliceous spheres and thin, tapered wollastonite blades precipitated from the fluid during the quench. For this reason the weight losses of the inner capsules gave lower limits to wollastonite solubility. In most quenched charges, essentially intact wollastonite crystals could be retrieved from the inner capsules. Small breakage losses from the irregularly dissolved crystals could give spuriously high solubility indication; for this reason the weights losses of the residual wollastonite crystals are regarded as giving upper solubility limits.

Some definitive runs on wollastonite solubility were on unencapsulated single crystals of the natural material whose initial weight was chosen to be close to the wollastonite solubility at a given NaCl concentration, as determined by the experiments on encapsulated crystals. The presence or absence of any residual crystals, as determined by observation of the quenched and dried charge with a binocular microscope, indicated whether the equilibrium fluid was wollastonite-saturated. In some experiments, it was possible to retrieve and weigh very small residual crystals, thus yielding a highly precise solubility value.

3. Results

3.1. Corundum

Measurements of the solubility of corundum in NaCl solutions at 10 kbar and 800 °C are listed in Table 1. The experiments were conducted for 3–7 days. This was deemed adequate for equilibrium based on comparison of our data in pure H_2O with the 12 h experiment of

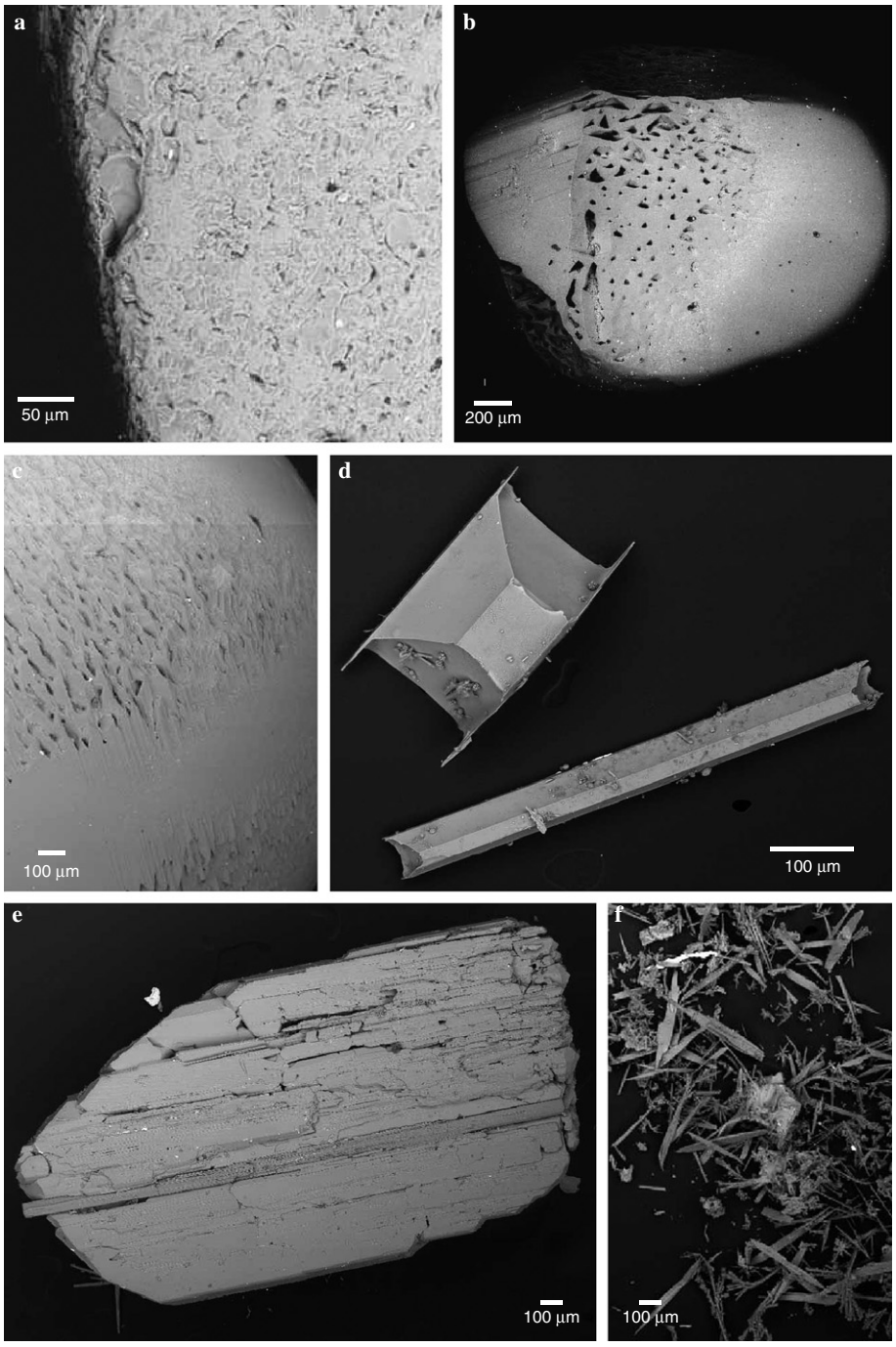

Fig. 1. Scanning-electron microscope images of starting materials and run products. (a) Surface appearance of rough-hewn synthetic corundum boule chip. (b) Facetted and etch-pitted surface of typical corundum crystal after dissolution experiment. (c) Etch-pitted surface of corundum sphere after dissolution experiment. (d) Two newly grown wollastonite crystals formed by vapor transport from the original encapsulated crystal over a small temperature gradient. Acicular whisker-like crystals are interpreted to be quench growth. (e) Residual wollastonite crystal after dissolution experiment. The crystal lost 93% of its mass in the experiment (WO-23, Table 1). (f) Insoluble quench-precipitate from wollastonite dissolution experiment after removal of quench-halite. Charge consists of bladed quench-wollastonite and myriad tiny siliceous spheres of vapor precipitate (“fish roe”).

Tropper and Manning (2005b), which indicates no detectable change in solubility at 800 °C, 10 kbar, from 12 to 168 h. The higher solubility of corundum in NaCl-bearing solutions and the evidence for substantial dissolution and reprecipitation, in the form of new crystal faces (Fig. 1b) and etch pits (Fig. 1c), further support the assumption of equilibrium.

The solubility of corundum in pure H_2O is very low at these conditions ($m_{Al_2O_3} = 0.0013(1)$, where m is mol/kg H_2O; Table 1). Al_2O_3 molality rises very rapidly with NaCl to $X_{NaCl} = 0.2$ (Fig. 2), but increases little further with X_{NaCl} from 0.2 to halite saturation (~0.58). Quenched solutions from corundum solubility runs at a range of X_{NaCl} had neutral pH (Table 1). Although it is likely that

Table 1
Experimental solubility measurements (800 °C, 10 kbar)

Expt. #	Time (h)	H_2O in mg	H_2O out mg	NaCl in mg	X_{NaCl}	Inner capsule in mg	Inner capsule out mg	Crystal in mg	Crystal out mg	Solubility (Δ_{cap}) mol/kg H_2O	Solubility (Δ_{xl}) mol/kg H_2O	Quench pH
Corundum (Al_2O_3)												
CB-16	168	35.719	35.776	0	0.000	—	—	0.466	0.461		0.0014(8)	
CB-19-*s*	161	36.791	na	0	0.000	—	—	32.6285	32.6236		0.0013(1)	7
CB-10	60	35.511	35.453	0.776	0.007	—	—	1.037	1.025		0.0033(8)	
CB-15	71	34.955	34.992	2.428	0.021	—	—	1.155	1.134		0.0059(8)	
CB-9	96	35.091	35.516	5.870	0.049	—	—	1.268	1.237		0.0087(8)	
CB-20-*s*	88	35.887	35.928	12.894	0.100	—	—	32.5904	32.5581		0.0088(1)	
CB-7	106	35.658	35.595	19.426	0.144	—	—	5.278	5.236		0.0116(8)	
CB-18-*s*	92	29.764	29.776	28.354	0.227	—	—	32.8928	32.8565		0.0120(1)	
CB-6	74	30.139	30.099	42.975	0.305	—	—	2.966	2.923		0.0140(9)	
SI-35	70	23.318	na	50.371	0.400	—	—	5.996	5.962		0.0143(12)	7
CB-8	71	21.688	21.247	61.120	0.470	—	—	2.857	2.827		0.0136(13)	
SI-44	74	12.692	na	48.320	0.540	—	—	5.671	5.652		0.0147(22)	7
SI-34-*h*	71	11.796	na	66.503	0.58(2)	—	—	6.014	5.995		0.0158(24)	7
Wollastonite ($CaSiO_3$)												
WO-16	6	36.517	na	0	0	72.702	72.6333	0.9189	0.8461	0.0162(7)	0.0172(1)	9
WO-1	17	34.615	34.655	0	0	76.201	76.133	4.000	3.909	0.017(1)	0.023(1)	
WO-17	30	36.759	na	3.695	0.030	64.068	63.8106	0.7398	0.4763	0.0603(7)	0.0617(1)	11
WO-5	21	33.260	33.105	7.036	0.061	69.961	69.631	1.722	1.358	0.085(1)	0.094(1)	
WO-13	2	37.824	37.907	13.628	0.100	81.3427	80.9429	1.1992	0.757	0.0910(6)	0.1006(1)	
WO-12	4	36.637	36.705	13.191	0.100	77.4251	76.9564	1.8526	1.3583	0.1101(7)	0.1161(1)	
WO-9	9	36.996	37.001	13.406	0.100	82.1607	81.6358	1.1913	0.6244	0.1221(7)	0.1319(1)	
WO-11	15	36.530	na	13.172	0.100	83.6195	83.119	1.4747	0.9503	0.1179(7)	0.1236(1)	11
WO-8	23	35.790	na	12.902	0.100	67.7113	67.1733	1.5628	1.0074	0.1294(7)	0.1336(1)	11
WO-22	30	34.594	34.587	12.532	0.100	71.1441	70.646	0.8966	0.3721	0.1240(7)	0.1305(1)	
WO-14	36	35.666	35.762	12.821	0.100	70.686	70.1404	1.066	0.498	0.132(1)	0.137(1)	
WO-15	48	36.333	36.298	13.008	0.099	68.9637	68.4342	1.1092	0.5391*	0.1255(7)	0.1351(1)	
WO-10	59	35.546	35.535	12.795	0.100	65.5959	64.977	1.4405	0.799**	0.1499(7)	0.1554(1)	
WO-23	72	30.934	31.135	11.156	0.100	—	—	0.5096	0.0364		0.1317(1)	
WO-7	89	37.212	na	13.370	0.100	80.1412	79.562	0.9698	0.3276*	0.1340(7)	0.1486(1)	
WO-4	22	26.567	26.497	14.66	0.145	72.271	71.800	1.442	0.934	0.153(1)	0.165(1)	
WO-6	22	26.55	26.476	23.575	0.215	68.039	67.384	1.77	1.093	0.212(1)	0.220(1)	
WO-2	20	20.907	20.580	29.382	0.302	76.844	76.179	1.894	1.191	0.274(1)	0.289(1)	
WO-24	94	22.511	22.567	41.795	0.364	—	—	0.8967	None		>0.342(1)	
WO-18	96	20.085	20.056	37.390	0.365	86.8278	86.0756	3.1549	nw#	0.3224(12)		
WO-27	90	20.529	20.586	49.457	0.426	—	—	1.17917	0.17307		0.4219(1)	
WO-3	21	21.141	19.050	45.890	0.426	71.467	70.664	1.572	0.633#	0.363(1)	0.424(1)	
WO-19	100	15.239	15.324	45.950	0.482	74.7329	74.0304	2.9306	2.2128	0.3969(16)	0.4055(2)	
WO-26	87	14.894	14.869	56.457	0.539	—	—	0.9317	0.08194		0.4912(2)	
WO-20	165	11.862	11.845	47.371	0.552	73.8629	73.2254	1.5226	0.8643	0.4627(21)	0.4778(2)	
WO-25	94	13.956	13.962	56.648	0.556	—	—	0.9853	0.2195		0.4724(2)	
Quartz (SiO_2)												
QZB-83	4	30.643	na	20.376	0.170	—	—	2.3353	0.9332		0.7615(2)	7

Notes: "in" and "out" refer, respectively, to before and after experiment; "Δ_{cap}" and "Δ_{xl}" denote changes in weight of inner capsule and crystal; "na," not analyzed; *, vapor-transport crystals present and included in crystal-out weight; **, vapor-transport crystals present but unweighable; "s," corundum sphere; "h," halite saturated experiment, as indicated by large (unweighed) halite cube in run product (X_{NaCl} taken from Newton and Manning, 2000); "none," crystal dissolved completely and solubility is minimum only; #, run product crystal was broken ("nw," not weighable). Weights given to three decimal places were determined using a Mettler M3 microbalance ($1\sigma = 2$ μg), whereas those to 4 decimal places made with a Mettler UMX2 ultramicrobalance ($1\sigma = 0.2$ μg). Parenthetical numbers denote propagated 1σ uncertainty in last decimal place. Maximum calculated 1σ in X_{NaCl} is 5×10^{-5}, except for experiment SI-34, for which stated uncertainty reflects the estimated accuracy at halite saturation (Aranovich and Newton, 1996; Newton and Manning, 2000).

some re-equilibration took place during and after the quench, this result shows that the dissolution reaction does not generate major amounts of either H^+ or OH^-.

We found that the two experiments with corundum spheres at $X_{NaCl} > 0$ yielded slightly lower solubility than the abraded boule-crystals at similar fluid composition (Fig. 2). Corundum spheres from these runs showed discrete bands and patches of etch pits which must reflect differential solubility as controlled by crystallography. In addition, one of the quenched spheres (Run CB-18, Table 1) showed very small Pt crystals on undissolved surfaces, presumably from vapor transport of Pt by the chloride solution. In contrast, boule chips show substantially greater recrystallization on all surfaces and did not have Pt

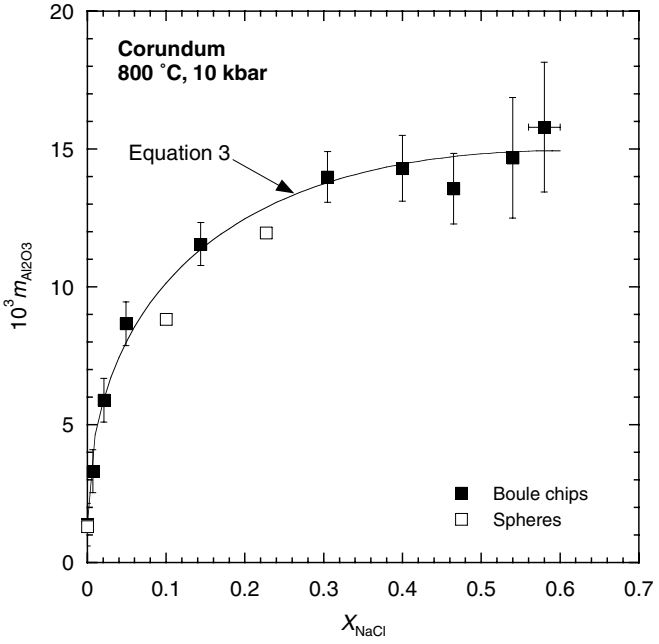

Fig. 2. Molality of Al_2O_3 vs. X_{NaCl} in corundum solubility experiments at 800 °C, 10 kbar. Error bars are 1σ propagated from weighing uncertainties. Solid squares are boule-chip data; open squares show results from corundum sphere experiments. The solubility behavior of the spheres in NaCl solutions may be significantly different from the rough-hewn crystals (see text) and were omitted from consideration during fitting and modeling. Solid line is empirical fit (Eq. (3)).

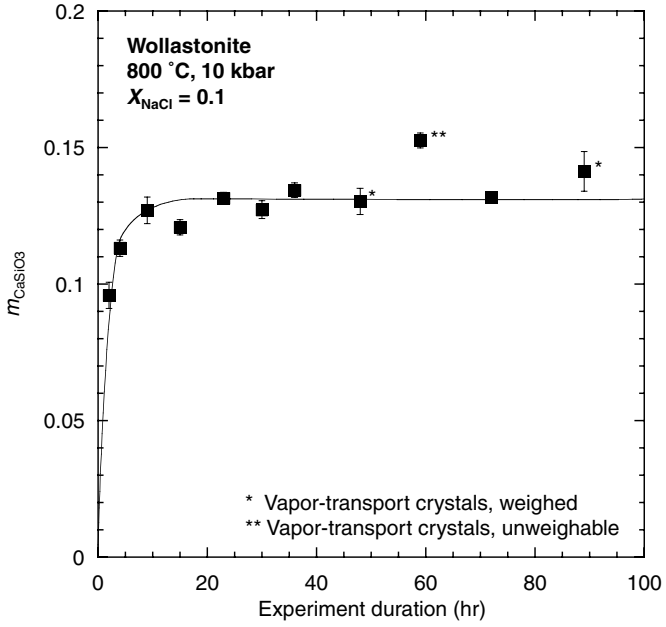

Fig. 3. Wollastonite solubility as a function of experiment duration at $X_{NaCl} = 0.1$, 800 °C, 10 kbar. Error bars give range between miminum and maximum values (Table 1), and solid squares plotted at midpoints. Time-independent $CaSiO_3$ molality values are attained after about 20 h. Experiments longer than about 50 h typically result in vapor-transported crystals of wollastonite outside of the inner capsule. In two experiments the vapor-transported crystals could be collected and weighed with the inner capsule to obtain a valid measurement. The precise measurement at 72 h (WO-23, Table 1) was from an experiment of an unencapsulated crystal whose initial mass barely exceeded the solubility limit. A very small residual crystal was identified in the quenched charge and weighed to give the precise molality value.

crystals. As weight changes could not be attributed solely to corundum dissolution in all experiments on spheres, we placed greater emphasis on the results from boule chips.

As shown in Fig. 2, the data for corundum solubility based on the boule-chip experiments alone are well-described by the empirical relation:

$$m_{Al_2O_3} = 0.001373 - 0.02227X_{NaCl} + 0.03477X_{NaCl}^{1/2} \quad (3)$$

3.2. Wollastonite

Results of wollastonite solubility measurements are given in Table 1. Equilibration times were evaluated at $X_{NaCl} = 0.1$. Fig. 3 shows that time-independent solubility measurements are attained after ~20 h at $X_{NaCl} = 0.1$. Runs at 6 and 17 h in pure H_2O support this conclusion. These results and the presence of new facets on residual wollastonite crystals (Fig. 1e) give assurance of a close approach to equilibrium solubility.

A complication in experiments at $X_{NaCl} < 0.2$ was that one or a few large limpid euhedral wollastonite crystals sometimes nucleated and grew at one end of the outer capsule (Fig. 1d). The new crystals are distinctly different from quench material in texture and abundance (Fig. 1f). Such crystals have been noted in other solubility studies (Caciagli and Manning, 2003; Tropper and Manning, 2005a). The crystals are interpreted to have grown by material transport by the fluid ("vapor transport") during the experiment due to small T gradients in the capsule. At $X_{NaCl} = 0.1$ (Fig. 3), runs longer than about 50 h result in vapor transport of wollastonite, with larger uncertainties in the measurements and a tendency toward spuriously high solubility values. In one experiment (WO-10, Table 1), there were many small vapor-transport crystals, too numerous to collect and weigh, yielding the spuriously high solubility (Fig. 3). In two other experiments, there were one or two obvious vapor-transport crystals, which could be collected and weighed with the inner capsule, but with greater uncertainty than other measurements. An attempt to define an upper solubility limit in a long run was made by introducing an unencapsulated crystal whose weight very slightly exceeded the solubility as averaged in the definitive shorter runs. Visual detection of a residual or vapor-transported crystal would place a firm upper limit on the solubility. This run of 72 h (WO-23, Table 1), was highly successful: a very small, highly corroded residual crystal was retrieved from the quenched and dried charge, and there were no vapor-transport crystals. The weight of the residual crystal gave a very precise solubility measurement confirming the value based on averaging the other data. Runs up to 7 days in length at $X_{NaCl} = 0.55$ did not yield vapor-transport crystals, probably because of the high heat-transporting capability of ionized salt, which minimized temperature gradients across the outer capsule.

Our results indicate that wollastonite is much less soluble than enstatite ($MgSiO_3$) in pure H_2O at 800 °C and 10 kbar (Newton and Manning, 2002) and, unlike enstatite, dissolves congruently. Fig. 4 shows that the wollastonite molality determined in the present study (0.0167 ± 0.005 molal) is significantly lower than the value of 0.0871 of by Fockenberg et al. (2006). We speculate that the higher value might be explained by vapor-transport crystals in the experiments of Fockenberg et al. (2006). Wollastonite solubility increases strongly with X_{NaCl}, rising nearly 40-fold between pure H_2O and halite saturation (Fig. 4). At high NaCl concentration, the silica concentrations are 2.5 times greater than at quartz saturation in the system H_2O–NaCl–SiO_2 at the same P and T (Newton and Manning, 2000). The solubility data can be described with high fidelity by:

$$m_{CaSiO_3} = 0.0204 + 0.6734X_{NaCl} + 0.1183X_{NaCl}^{1/2} \quad (4)$$

(Fig. 4). The data appear to be more scattered at $X_{NaCl} > 0.3$, possibly from greater difficulty of equilibration in the high-NaCl, low-H_2O fluids, but more probably because of the very high solubilities, and hence congestion of the recovered charges with quenched fluid precipitate.

Measurements of pH of fluids quenched from wollastonite solubility experiments were strongly basic. The pure H_2O runs gave a pH of about 9, whereas all NaCl-bearing charges yielded a pH of 11. This result indicates that OH^- is a major product of the dissolution reaction and is enhanced by the presence of NaCl.

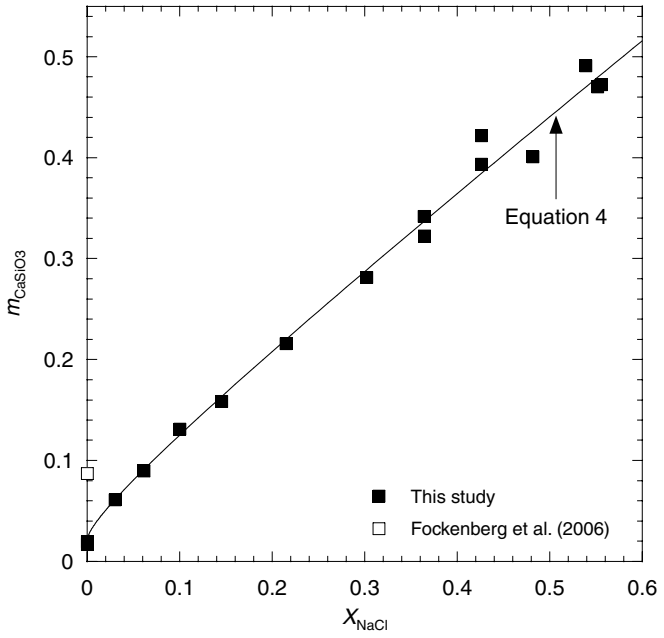

Fig. 4. Molality of $CaSiO_3$ vs. X_{NaCl} in wollastonite solubility experiments at 800 °C, 10 kbar. Data (solid squares) and error bars plotted as in Fig. 3, except datum at $X_{NaCl} = 0.1$, which is the weighted average of experiments >20 h and lacking vapor-transport crystals (Table 1; Fig. 3). Solid curve is Eq. (4). Open square shows measurement of Fockenberg et al. (2006).

3.3. Quartz

Newton and Manning (2000) measured quartz solubility in H_2O–NaCl solutions at 10 kbar and 800 °C in H_2O–NaCl (Fig. 5). We conducted an additional experiment at $X_{NaCl} = 0.17$ to evaluate quench pH, which is 7 (Table 1). This suggests that any solvent interaction similar to that of Eq. (1) is quite negligible at these elevated P–T conditions.

The effect of NaCl on quartz solubility at high pressures and temperatures (Fig. 5) contrasts with that on corundum and wollastonite: the monotonic decline in quartz solubility with X_{NaCl} indicates that decrease of H_2O activity is a greater factor in solubility than solvent interaction. As discussed above, quartz shows different behavior at low P, where an initial enhancement of quartz solubility with increasing X_{NaCl} at $\leqslant 2$ kbar indicates substantial interaction between the solvent and dissolved silica.

4. Discussion

The contrasting dependence of solubility of corundum, wollastonite and quartz on X_{NaCl} can be explored using a simple ideal-fused-salt model. It is useful as a first step to convert concentrations from molality (Table 1) to the mole fraction scale, the formulation of which depends on the state of the solvent. Aranovich and Newton (1996) showed

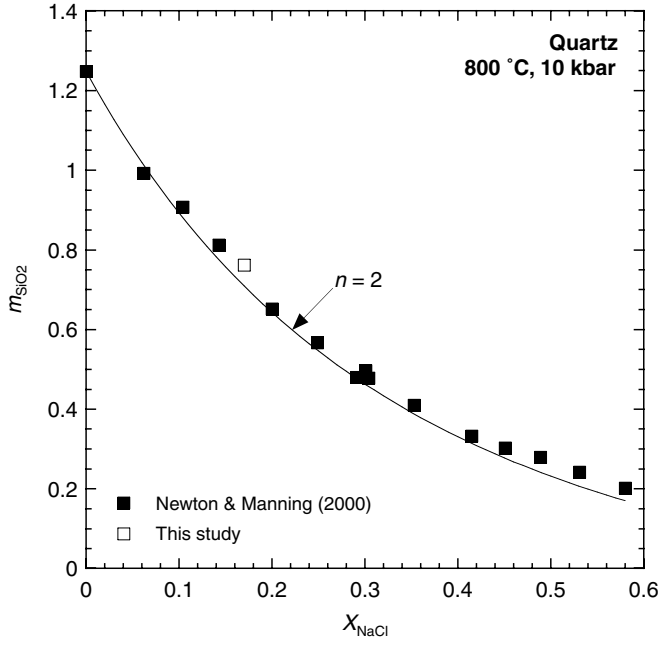

Fig. 5. Molality of SiO_2 vs. X_{NaCl} in quartz solubility experiments at 800 °C, 10 kbar. Filled squares are from Newton and Manning (2000); open square, this study. Solid line is a theoretical curve using the SiO_2 polymerization theory of Newton and Manning (2003) with a monomer hydration number (n) of 2 and $K_{md} = 118$ (see text). The good agreement between the experimental data and the prediction with $n = 2$ implies that SiO_2 species in NaCl solutions at 800 °C and 10 kbar have negligible hydrogen-bonded H_2O of solvation at high temperature and pressure.

experimentally that H_2O and NaCl mix in all proportions at 800 °C and 10 kbar as if these solutions were ideal mixtures of Na^+ and Cl^- ions and H_2O molecules. Following Bradley (1962), the mole fraction of species i among j total species (ions or molecules) is $X_i = n_i/\sum_j n_j$, where n is number of moles and electrical neutrality is maintained (see also Pitzer, 1980; Pabalan and Pitzer, 1990). Thus, $X_{H_2O} = 0.33$ in an equimolar mixture of H_2O and fully dissociated NaCl (ions produced by minor H_2O dissociation are clearly negligible). Implicit in Bradley's treatment are standard states of unit activity at any P and T of pure solids (halite), liquids (H_2O) and fully dissociated fused salts (liquid NaCl), which leads directly to Eqs. (2a) and (2b). Assuming that solute concentrations derived from congruently dissolving mineral r (quartz, corundum or wollastonite) are small, their unknown extent of dissociation and degree of interaction with Na, Cl, and H_2O can be ignored, and mole fraction can be calculated from molality from

$$X_r = \frac{m_r}{m_r + 55.51\left(1 + \frac{2X_{NaCl}}{1-X_{NaCl}}\right)} \tag{5}$$

where X_{NaCl} is the mole fraction of NaCl in the H_2O–NaCl subsystem.

Fig. 6 shows that, when compared to their values in pure H_2O, mole fractions of solutes in H_2O–NaCl fluid coexisting with corundum, wollastonite or quartz display important differences in their changes with X_{NaCl}. Wollastonite shows strong relative solubility enhancement with NaCl,

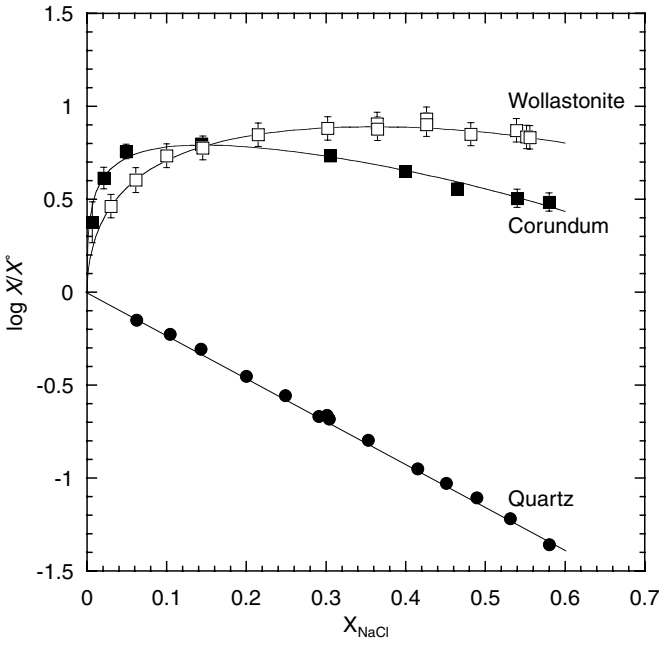

Fig. 6. Solubility enhancement factors of quartz, corundum and wollastonite in NaCl–H_2O solutions at 800 °C and 10 kbar, expressed as the log of the ratio of mole fraction at a given NaCl concentration to that in pure H_2O (X_i/X_i°). Mole fractions calculated assuming complete dissociation of NaCl to Na^+ and Cl^- (Eq. (5)). The curves show the empirical fits to the corundum (Eq. (3)) and wollastonite (Eq. (4)) solubility data. Quartz solubility data from Newton and Manning (2000).

rising rapidly with salinity to a concentration at halite saturation of about 40 times the pure H_2O value, though the H_2O content is only 17 wt%. Corundum shows an even more drastic initial enhancement, but reaches a maximum at a NaCl mole fraction of about 0.15, and then begins to decline slowly. Quartz solubility decreases monotonically to halite saturation. Below we dicuss implications of these observations.

4.1. Quartz

The decrease in quartz solubility with NaCl concentration (Fig. 6) suggests that there is no interaction between NaCl and aqueous SiO_2. A negative correlation between solubility and H_2O concentration further suggests that dissolved solutes are hydrous molecules. Inasmuch as Aranovich and Newton (1996) found that Na^+, Cl^- and H_2O closely approximate an ideal solution at 800 °C, 10 kbar, and Newton and Manning (2003) observed that dissolved SiO_2 in H_2O could successfully be modeled using an ideal mixing approximation for silica monomers and dimers, we hypothesize that a simple ideal solution approach can be extended to quartz-saturated solutions in the ternary SiO_2–H_2O–NaCl system. To assess the validity of this hypothesis, we follow the approach of Walther and Orville (1983), who estimated the hydration number n of monomeric solute silica, $SiO_2 \cdot nH_2O$, in equilibrium with quartz at elevated T and P via

$$\underset{\text{quartz}}{SiO_2} + nH_2O = \underset{\text{monomer}}{SiO_2 \cdot nH_2O} \tag{6}$$

for which the equilibrium constant, K_{qm}, is

$$K_{qm} = \frac{a_s}{a_{H_2O}^n} \tag{7}$$

where a_s is the activity of aqueous silica monomers. Eq. (7) leads to the linear relation

$$\log a_s = n \log a_{H_2O} + \log K_{qm} \tag{8}$$

Assuming that a_s was equal to the molality of total dissolved silica, m_s, and that $a_{H_2O} = X_{H_2O}$, Walther and Orville (1983) used quartz solubility data of their own and others in CO_2–H_2O and Ar–H_2O solutions to construct plots of $\log m_{SiO_2}$ vs. $\log X_{H_2O}$ at P–T conditions up to 5 kbar and 700 °C. If m_s is an adequate representation of silica activity and if hydroxyl H_2O and hydrogen-bonded H_2O are considered thermodynamically equivalent, the slope of a solubility isotherm at constant pressure defines n per SiO_2 unit. Walther and Orville found that n was between 3 and 5 for the available solubility data.

The approach of Walther and Orville (1983) can be improved by a more exact formulation of H_2O and silica activities. As described above, H_2O activity in H_2O–NaCl solutions is closely approximated by Eq. (2a) at 800 °C, 10 kbar (Aranovich and Newton, 1996), provided solute concentrations are low ($X_r < 0.01$). Silica activity can be calculated using the approach of Newton and Manning (2003), which accounts for polymerization of aqueous

silica. At the conditions of the present study, dissolved silica in pure H_2O occurs primarily as two hydrous species, monomers and dimers (Zhang and Frantz, 2000; Zotov and Keppler, 2000, 2002; Newton and Manning, 2002, 2003). Other species likely occur as well, but these evidently contribute negligibly to the total Gibbs free energy of solute silica. The equilibrium governing formation of a dimer molecule ($H_6Si_2O_7$) from two monomers (H_4SiO_4) can be written as

$$\underset{\text{monomer}}{2SiO_2 \cdot nH_2O} = \underset{\text{dimer}}{Si_2O_4 \cdot (2n-1)H_2O} + H_2O \quad (9)$$

where n is the number of moles of H_2O per mole of monomeric silica, including both hydroxyls and solvated molecular H_2O. If some of the bound H_2O are indeed solvated (hydrogen-bonded rather than hydroxyl), the assumption is implicit that the solvation per SiO_2 molecule is the same in both monomer and dimer. Following Newton and Manning (2002, 2003), we adopt a standard state for aqueous silica of unit activity of the pure hypothetical solution of silica monomers referenced to infinite dilution, and assume ideal mixing of monomers and dimers. This leads to expression of the equilibrium constant for Eq. (9) as

$$K_{md} = \frac{X_d a_{H_2O}}{X_m^2} \quad (10)$$

where subscripts m, d and md denote, respectively, monomer, dimer and monomer–dimer equilibrium, and mole fractions are calculated as in Eq. (5). In this approach, the total solute silica activity, a_s, is equal to the mole fraction of monomers.

$$a_s = \gamma_s X_s = X_m \quad (11)$$

where γ_s, is the activity coefficient of solute silica. Combination of Eqs. (10) and (11) leads to

$$a_s = \frac{(1 + 8X_s K_{md}/a_{H_2O})^{1/2} - 1}{4K_{md}/a_{H_2O}} \quad (12)$$

(Newton and Manning, 2002, 2003). Eq. (12) permits direct assessment of the change in the activity of silica in quartz-saturated H_2O–NaCl solutions with a_{H_2O} (Eq. (8)).

Fig. 7 shows that there is strong, linear correlation between the logarithm of silica activity on a_{H_2O}, using $K_{md} = 118$ (Zotov and Keppler, 2002). Linear regression yields $n = 1.88$ ($R = 0.9995$), very close to 2. Given that $n = 2$ corresponds to H_4SiO_4 and $H_6Si_2O_7$, this result suggests that solvated molecular H_2O is thermodynamically negligible at 800 °C,10 kbar, in H_2O–NaCl, and that interaction energies between molecules and ions of the bulk solvent (H_2O, Na^+, and Cl^-) and the silica species are very small; i.e., the solution closely approaches ideality. Possible sources of error include uncertainty in K_{md}, as well as the assumption of complete dissociation of NaCl.

The utility of the observation of $n \sim 2$ is that it permits prediction of quartz solubility in H_2O–NaCl solutions without any additional fit parameters. Fig. 5 gives predicted quartz solubility derived by rearranging Eq. (12), with

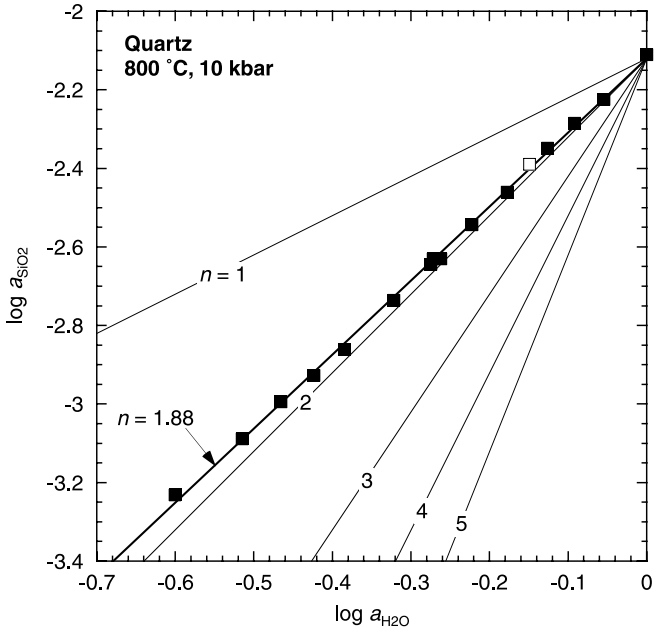

Fig. 7. Variation in SiO_2 activity with a_{H_2O} at 800 °C, 10 kbar. Silica activity calculated from quartz solubility data (Newton and Manning, 2000; Table 1) by Eq. (12) (see text). A linear fit gives $R = 0.9995$) with a slope of 1.88, which gives the hydration number n (Eq. (8)). Also shown are a range in integer hydration numbers, illustrating the close approach to $n = 2$. The result indicates that the hydrogen-bonded H_2O per SiO_2 unit is negligible; that is, that the monomer and dimer have forumulas, respectively, of H_4SiO_4 and $H_6Si_2O_7$. In contrast, Walther and Orville (1983) found that solute silica in H_2O–CO_2 and H_2O–Ar fluids at pressures to 4 kbar and temperatures to 700 °C has 1–3 hydrogen-bonded H_2O per SiO_2 unit.

(1) quartz solubility in pure H_2O (Table 1), (2) $K_{md} = 118$ (Zotov and Keppler, 2002), and (3) H_2O activity calculated from Eq. (2). It can be seen that adopting $n = 2$ closely reproduces the experimental data.

The foregoing suggests that, to a first approximation, dissolution of quartz in H_2O–NaCl mixtures behaves as if there were ideal solution of all neutral molecules and ions, consonant with the findings of Aranovich and Newton (1996) for the system NaCl–H_2O and of Newton and Manning (2003) for SiO_2 solutions of various activities in H_2O at high temperature and pressure. It is not clear why hydrogen bonding of H_2O to silica should be inhibited in NaCl–H_2O, while it is significant in CO_2–H_2O and Ar–H_2O solutions at high P and T. Apparently, the presence of dissociated Na^+ and Cl^- ions alters the electrical environment of the fluid in a way that is inimical to hydrogen bonding.

4.2. Corundum

In contrast to H_2O–NaCl solutions in equilibrium with quartz, the identities and number of dominant solute species coexisting with corundum and wollastonite are unconstrained. This precludes direct application of the simple model described above. However, Fig. 6 nevertheless offers some insight into the nature of the dominant species. If one

mole of corundum reacts with A moles of NaCl and B moles of H_2O to produce k moles of solutes, then we can write

$$\underset{\text{corundum}}{Al_2O_3} + A\text{NaCl} + B\text{H}_2\text{O} = k \text{ solutes} \quad (13)$$

If corundum solubility decreased with X_{NaCl}, as does quartz, then Al solutes would likely be hydrous species, and there would be no interaction with Na^+ and/or Cl^-. Similarly, monotonic increase with X_{NaCl} would imply no interaction with H_2O. However, Fig. 6 shows that corundum solubility increases to a maximum and then declines. This behavior strongly implies that Al solutes include both hydrates and Na- and/or Cl complexes: the enhancement effect of complex formation is eventually overtaken by progressive destabilization of hydrous species as H_2O activity decreases. The solubility maximum near $X_{NaCl} \sim 0.15$ suggests that the ratio of H_2O to NaCl absorbed in the dissolution reaction is about 6; that is, B:A in Eq. (13) is about 6:1.

Reaction (13) with parameters A and B set at 1 and 6, respectively, may be tentatively interpreted in terms of actual dissolution reactions. It may be supposed that an Na–Al interaction product is the neutral hydrous molecule, $NaAl(OH)_4$ (Anderson and Burnham, 1967; Walther, 2001). A model reaction which satisfies the above choice of parameters is

$$\underset{\text{corundum}}{2Al_2O_3} + \text{NaCl} + 6\text{H}_2\text{O} = \text{NaAl(OH)}_4 + \text{Al(OH)}_2\text{Cl} + 2\text{Al(OH)}_3 \quad (14)$$

An equally consistent reaction in terms of ions is:

$$\underset{\text{corundum}}{Al_2O_3} + \text{Na}^+ + 3\text{H}_2\text{O} = \text{NaAl(OH)}_4 + \text{Al(OH)}_2^+ \quad (15)$$

Both postulated reactions satisfy the inferred stoichiometric parameters and the experimental finding that H^+ and OH^- are not major products.

4.3. Wollastonite

Fig. 6 shows that wollastonite solubility displays a broad maximum near $X_{NaCl} \sim 0.33$, implying that dissolution consumes H_2O and NaCl in the ratio 2:1. The great solubility enhancement of wollastonite by NaCl implies that a solute Ca chloride species is formed, and the very basic nature of the quenched fluids requires that OH^- is a major product of the dissolution reaction. A simple—though nonunique—dissolution reaction which satisfies the above criteria is:

$$\underset{\text{wollastonite}}{CaSiO_3} + \text{NaCl} + 2\text{H}_2\text{O} = \text{CaCl}^+ + \text{OH}^- + \text{H}_3\text{NaSiO}_4 \quad (16)$$

The neutral silicate species, originally proposed by Anderson and Burnham (1967), is required to preserve charge balance and accommodate the H, Na and SiO_2 left over from the formation of $CaCl^+$ and OH^-. Formation of significant H_3NaSiO_4 in the wollastonite experiments but not in the quartz experiments could result from the strong interactions of Ca^{+2} and Cl^-, and explain our observation that, near halite saturation, the silica content of brines coexisting with wollastonite is higher than those with quartz.

5. Conclusions

Interaction of crustal and upper mantle rocks with fluids of magmatic or metamorphic origin are complex, involving polymerization, hydration and dehydration, ionization, acid/base relations, etc. These complexities are compounded by the inevitable tendency of deep-seated fluids to rise, with attendant decrease of temperature and pressure, thus with continuous alteration of the fluids and their host rocks as they ascend. In the present limited assessment of interaction of saline fluids with three congruently soluble simple minerals, we have found greatly diverse behavior, as shown in Fig. 6. Wollastonite shows strong relative solubility enhancement with NaCl, with a concentration at halite saturation of about 40 times the pure H_2O value, though the H_2O content is only 17 wt%. The solubility relative to pure H_2O shows a broad maximum at $X_{NaCl} \sim 0.33$. Corundum shows an even more drastic initial enhancement, but reaches a maximum at a NaCl mole fraction of about 0.15, and then begins to decline slowly. Quartz solubility decreases monotonically to halite saturation.

In spite of the diverse behavior shown by Fig. 6, the solubilities of quartz, corundum and wollastonite can perhaps be understood with a simple model in which solute products mix ideally with all ions and neutral molecules. These aspects include solvent interactions, the role of H_2O activity, hydration and ionization states of solute products, and acid/base relationships. Interpretation of the shapes of the salinity–solubility curves, together with the pH of quenched solutions, yields the following preliminary conclusions:

1. *Quartz* dissolves to mixtures of silica monomers, H_4SiO_4, and dimers, $H_6Si_2O_7$, their relative proportions depending on T, P, and X_{NaCl}. Additional H_2O of solvation is probably negligible at 800 °C and 10 kbar, as are Na-silicate species. Quenched experimental solutions were pH-neutral. At upper crustal pressures of 1–2 kbar, however, Na-silicate species are likely, and H_2O solvation is greater.
2. *Corundum* dissolves to a hydrous Na–aluminate complex, possibly $NaAl(OH)_4$. Certain amounts of other Al species, probably hydroxides, must be yielded in order to balance a dissolution reaction without major H^+ or OH^-. It is probable that addition of SiO_2 to the system H_2O–NaCl–Al_2O_3 would yield Na–aluminosilicate complexes, as advocated by Anderson and Burnham (1983), and thus would generate strongly acid solutions.
3. *Wollastonite* dissolves to a Ca chloride, probably $CaCl^+$, with equal amounts of OH^- for charge balance. The SiO_2 may be accommodated as a neutral Na-silicate

complex, such as H_3NaSiO_4. The NaCl enhancement effect on $CaSiO_3$ solubility is so great at 10 kbar and 800 °C that, at NaCl conditions near halite saturation, the silica concentration is more than double that of quartz saturation in the system SiO_2–NaCl–H_2O.

An important project for further investigation would be to add SiO_2 to the system $CaSiO_3$–NaCl–H_2O, in order to determine whether relative amounts of the postulated species H_4SiO_4, $H_6Si_2O_7$, $CaCl^+$, OH^-, and H_3NaSiO_4 are predictable in the larger system. A similarly pertinent investigation concerns addition of quartz to the Al_2O_3–NaCl–H_2O system, in the attempt to define Na–aluminosilicate species and acid-base relationships. According to Anderson and Burnham (1983), Al_2O_3 is very soluble in quartzofeldspathic compositions as feldspar-like vapor species. Solubility studies in the combined system $CaSiO_3$-Al_2O_3–NaCl–H_2O, with special reference to grossular garnet ($Ca_3Al_2Si_3O_{12}$) would be a logical continuation of the present study. These extended studies could provide a framework for analysis of the solubility behavior of more complex systems, emulating common rocks. It might happen that the simple solution behavior found in the present study on individual minerals could be extended to assemblages of several minerals in more tractable ways than have been previously recognized.

Acknowledgments

This research was supported by National Science Foundation grant EAR-0337170 to CEM. Bruce Yardley, John Walther and Dimitri Sverjensky provided helpful reviews of an earlier version of the manuscript. Walther's detailed comments in particular resulted in substantial changes in the paper. We thank Jeremy Wykes and Peter Tropper for assistance with SEM imaging.

Associate editor: Dimitri A. Sverjensky

References

Ague, J.J., 1994. Mass-transfer during Barrovian metamorphism of pelites, south-central Connecticut. I: evidence for changes in composition and volume. *American Journal of Science* **294**, 989–1057.

Anderson, G.M., Burnham, C.W., 1967. Reaction of quartz and corundum with aqueous chloride and hydroxide solutions at high temperatures and pressures. *American Journal of Science* **265**, 12–27.

Anderson, G.M., Burnham, C.W., 1983. Feldspar solubility and the transport of aluminum under metamorphic conditions. *American Journal of Science* **283-A**, 283–297.

Aranovich, L.Y., Newton, R.C., 1996. H_2O activity in concentrated NaCl solutions at high pressures and temperatures measured by the brucite–periclase equilibrium. *Contributions to Mineralogy and Petrology* **125**, 200–212.

Aranovich, L.Y., Newton, R.C., 1997. H_2O activity in concentrated KCl and KCl–NaCl solutions at high temperatures and pressures measured by the brucite–periclase equilibrium. *Contributions to Mineralogy and Petrology* **127**, 261–271.

Aranovich, L.Y., Newton, R.C., 1998. Reversed determination of the reaction: phlogopite + quartz = enstatite + potassium feldspar + H_2O in the range 750–875 °C and 2–12 kbar at low H_2O activity with concentrated KCl solutions. *American Mineralogist* **83**, 193–204.

Aranovich, L.Y., Shmulovich, K.I., Fedkin, V.V., 1987. The H_2O and CO_2 regime in regional metamorphism. *International Geology Review* **29**, 1379–1401.

Bowers, T.S., Helgeson, H.C., 1983. Calculation of the geochemical consequences of non-ideal mixing in the system H_2O–CO_2–NaCl in geologic systems: equation of state of H_2O–CO_2–NaCl fluids at high pressures and temperatures. *Geochimica et Cosmochimica Acta* **47**, 1247–1275.

Bradley, R.S., 1962. Thermodynamic calculations on phase equilibria involving fused salts. Part I. General theory and application to equilibria involving calcium carbonate at high pressure. *American Journal of Science* **260**, 374–382.

Caciagli, N.C., Manning, C.E., 2003. The solubility of calcite in water at 5–16 kbar and 500–800 °C. *Contributions to Mineralogy and Petrology* **146**, 275–285.

Cameron, E.M., Hattori, K., 1994. Highly oxidized deep metamorphic zones: occurrence and origin. *Mineralogical Magazine* **58A**, 142–143.

Charlu, T.V., Newton, R.C., Kleppa, O.J., 1978. Enthalpy of formation of some lime silicates by high-temperature solution calorimetry, with discussion of high pressure phase equilibria. *Geochimica et Cosmochimica Acta* **42**, 367–375.

Crawford, M.L., Hollister, L.S., 1986. Metamorphic fluids, the evidence from fluid inclusions. In: Walther, J.V., Wood, B.J. (Eds.), *Fluid–rock Interactions During Metamorphism*. Springer, New York, pp. 1–35.

Fockenberg, T., Burchard, M., Maresch, W.V., 2006. Experimental determination of the solubility of natural wollastonite in pure water up to pressures of 5 GPa and at temperatures of 400–800 °C. *Geochimica et Cosmochimica Acta* **70**, 1796–1806.

Gibert, F., Guillaume, D., LaPorte, D., 1998. Importance of fluid immiscibility in the H_2O–NaCl–CO_2 system and selective CO_2 entrapment in granulites: experimental phase diagram at 5–7 kbar, 900 °C and wetting textures. *European Journal of Mineralogy* **10**, 1109–1123.

Johnson, E.L., 1991. Experimentally determined limits for H_2O–CO_2–NaCl immiscibility in granulites. *Geology* **19**, 925–928.

Kennedy, G.C., 1950. A portion of the system silica–water. *Economic Geology* **45**, 629–653.

Lamb, W., Valley, J.W., 1984. Metamorphism of reduced granulites in low-CO_2 vapour-free environment. *Nature* **312**, 56–58.

Manning, C.E., Ingebritsen, S.E., 1999. Permeability of the continental crust: constraints from heat flow models and metamorphic systems. *Reviews in Geophysics* **37**, 127–150.

Newton, R.C., Manning, C.E., 2000. Quartz solubility in H_2O–NaCl and H_2O–CO_2 solutions at deep crust-upper mantle pressures and temperatures: 2–15 kbar and 500–900 °C. *Geochimica et Cosmochimica Acta* **64**, 2993–3005.

Newton, R.C., Manning, C.E., 2002. Solubility of enstatite + forsterite in H_2O at deep crust/upper mantle conditions: 4 to 15 kbar and 700 to 900 °C. *Geochimica et Cosmochimica Acta* **23**, 4165–4176.

Newton, R.C., Manning, C.E., 2003. Activity coefficient and polymerization of aqueous silica at 800 °C, 12 kbar, from solubility measurements on SiO_2-buffered mineral assemblages. *Contributions to Mineralogy and Petrology* **146**, 135–143.

Newton, R.C., Manning, C.E., 2005. Solubility of anhydrite, $CaSO_4$, in NaCl–H_2O solutions at high pressures and temperatures: applications to fluid–rock interaction. *Journal of Petrology* **46**, 701–716.

Newton, R.C., Aranovich, L.Y., Hansen, E.C., Vandenheuvel, B.A., 1998. Hypersaline fluids in Precambrian deep-crustal metamorphism. *Precambrian Research* **91**, 41–63.

Novgorodov, P.G., 1977. On the solubility of quartz in H_2O + CO_2 and H_2O + NaCl at 700 °C and 1.5 kb pressure. *Geochemistry International* **14** (4), 191–193.

Pabalan, R.T., Pitzer, K.S., 1990. Models for aqueous electrolyte mixtures for systems extending from dilute solutions to fused salts. In: Melchior, D.C., Bassett, R.L. (Eds.), *Chemical Modeling of Aqueous Systems II*, 416. American Chemical Society Series, pp. 44–57.

Philippot, P., Selverstone, J., 1991. Trace-element-rich brines in eclogitic veins: implications for fluid composition and transport during subduction. *Contributions to Mineralogy and Petrology* **106**, 417–430.

Pitzer, K.S., 1980. Electrolytes. From dilute solutions to fused salts. *Journal of the American Chemical Society* **102**, 2902–2906.

Roedder, E., 1972. The composition of fluid inclusions. *U.S. Geological Survey Professional Paper 440JJ*, 1–64.

Shmulovich, K.I., Graham, C.M., 2004. An experimental study of phase equilibria in the systems H_2O–CO_2–$CaCl_2$ and H_2O–CO_2–NaCl at high pressures and temperatures (500–800 °C, 0.5–0.9 GPa): geological and geophysical applications. *Contributions to Mineralogy and Petrology* **146**, 450–462.

Shmulovich, K., Graham, C., Yardley, B., 2001. Quartz, albite and diopside solubilities in H_2O–NaCl and H_2O–CO_2 fluids at 0.5–0.9 GPa. *Contributions to Mineralogy and Petrology* **141**, 95–108.

Shmulovich, K.I., Yardley, B.W.D., Graham, C.M., 2006. Solubility of quartz in crustal fluids: experiments and general equations for salt solutions and H_2O–CO_2 mixtures at 400–800 °C and 0.1–0.9 GPa. *Geofluids* **6**, 154–167.

Smit, C.A., Van Reenen, D.D., 1997. Deep crustal shear zones, high-grade tectonites, and associated metasomatic alteration in the Limpopo Belt, South Africa. *Journal of Geology* **105**, 37–58.

Touret, J.L.R., 1971. Le faciès granulite en Norwège Méridionale. *Lithos* **4**, 239–249, see also pages 423–436.

Touret, J.L.R., 1985. Fluid regime in southern Norway, the record of fluid inclusions. In: Tobi, A.C., Touret, J.L.R. (Eds.), *The Deep Proterozoic Crust in the North Atlantic Provinces*. Reidel, Dordrecht, pp. 517–549.

Tropper, P., Manning, C.E., 2004. Paragonite stability at 700 °C in the presence of H_2O–NaCl fluids: constraints from H_2O activity and implications for high pressure metamorphism. *Contributions to Mineralogy and Petrology* **147**, 740–749.

Tropper, P., Manning, C.E., 2005a. Very low solubility of rutile in H_2O at high pressure and temperature, and its implications for Ti mobility in subduction zones. *American Mineralogist* **90**, 502–505.

Tropper, P., Manning, C.E., 2005b. The solubility of corundum in H_2O at high temperature and pressure, and its consequences for Al mobility in subduction zone environments. *Geophysical Research Abstracts* **7**, 03991.

Valley, J.W., McLelland, J., Essene, E.J., Lamb, W., 1983. Metamorphic fluids in the deep crust: evidence from the Adirondacks. *Nature* **301**, 226–228.

Valley, J.W., Bohlen, S.R., Essene, E.J., Lamb, W., 1990. Metamorphism in the Adirondacks: II: the role of fluids. *Journal of Petrology* **31**, 555–596.

Walther, J.V., 2001. Experimental determination and analysis of the solubility of corundum in 0.1 and 0.5 m NaCl solutions between 400 and 600 °C from 0.5 to 2.0 kbar. *Geochimica et Cosmochimica Acta* **65**, 2843–2851.

Walther, J.V., Orville, P.M., 1983. The extraction-quench technique for determination of the thermodynamic properties of solute complexes. Application to quartz solubility in fluid mixtures. *American Mineralogist* **68**, 731–741.

Xie, Z., Walther, J.V., 1993. Quartz solubilities in NaCl solutions with and without wollastonite at elevated temperatures and pressures. *Geochimica et Cosmochimica Acta* **57**, 1947–1955.

Zotov, N., Keppler, H., 2002. Silica speciation in aqueous fluids at high pressures and temperatures. *Chemical Geology* **184**, 71–82.